

Identification of Abnormal States in Videos of Ants Undergoing Social Phase Change

Taeyeong Choi^{1,2}, Benjamin Pyenson³, Juergen Liebig³, Theodore P. Pavlic^{2,3,4}

¹ Lincoln Institute for Agri-food Technology, University of Lincoln, Riseholme Park, Lincoln, UK

² School of Computing, Informatics, and Decision Systems Engineering, Arizona State University, Tempe, AZ, USA

³ School of Life Sciences, Arizona State University, Tempe, AZ, USA

⁴ School of Sustainability, Arizona State University, Tempe, AZ, USA

tchoi@lincoln.ac.uk, {bpyenson, jliebig, tpavlic}@asu.edu

Abstract

Biology is both an important application area and a source of motivation for development of advanced machine learning techniques. Although much attention has been paid to large and complex data sets resulting from high-throughput sequencing, advances in high-quality video recording technology have begun to generate similarly rich data sets requiring sophisticated techniques from both computer vision and time-series analysis. Moreover, just as studying gene expression patterns in one organism can reveal general principles that apply to other organisms, the study of complex social interactions in an experimentally tractable model system, such as a laboratory ant colony, can provide general principles about the dynamics of other social groups. Here, we focus on one such example from the study of reproductive regulation in small laboratory colonies of more than 50 *Harpegnathos* ants. These ants can be artificially induced to begin a ~20 day process of hierarchy reformation. Although the conclusion of this process is conspicuous to a human observer, it remains unclear which behaviors during the transient period are contributing to the process. To address this issue, we explore the potential application of One-class Classification (OC) to the detection of *abnormal* states in ant colonies for which behavioral data is only available for the *normal* societal conditions during training. Specifically, we build upon the Deep Support Vector Data Description (DSVDD) and introduce the Inner-Outlier Generator (IO-GEN) that synthesizes fake “inner outlier” observations during training that are near the center of the DSVDD data description. We show that IO-GEN increases the reliability of the final OC classifier relative to other DSVDD baselines. This method can be used to screen video frames for which additional human observation is needed. Although we focus on an application with laboratory colonies of social insects, this approach may be applied to video data from other social systems to either better understand the causal factors behind social phase transitions or even to predict the onset of future transitions.

Introduction

In natural social systems, complex interactions among large numbers of individuals can give rise to phenomena such as “collective minds” (Couzin 2007) and, as in colonies of

Copyright © 2021, Association for the Advancement of Artificial Intelligence (www.aaai.org). All rights reserved.

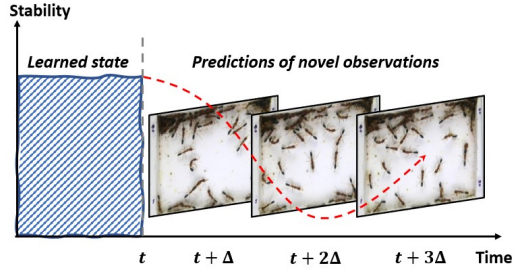


Figure 1: Proposed scenario in which observational data from an ant colony are accessible during its stable state, while the trained predictive model is to classify behaviors from unseen, unstable states.

ants, even “superorganisms” where the collective can be described as a single monolithic entity. Some ant species have colonies sufficiently small to be observed in their entirety with state-of-the-art video-recording technologies and sufficiently large to have rich, multi-scale behaviors. Whereas the dynamical processes underlying the non-trivial interactions between ants are cryptic to human observers, there is potential for machine-learning and artificial-intelligence techniques to identify social interaction patterns that warrant further study. For example, in species of ants where new reproductive individuals emerge after the previous reproductive dies naturally or is artificially removed (Heinze, Hölldobler, and Peeters 1994; Sasaki et al. 2016), machine learning could in principle help to identify abnormal patterns that only occur during this conflict resolution. However, such a behavioral classifier for underappreciated *abnormal* patterns would necessarily be limited to training data from videos of behaviors under known *normal* conditions.

Here, we propose an alternative application of One-class Classification (OC) to solve the *abnormal state detection problem* for video data of social systems in transition from disordered to ordered states. In these systems, behavioral data for training the classifier is only available for the system’s typical state, but the classifier must be able to classify abnormal samples presented to it after training. For OC problems, Support-Vector-Machine-inspired approaches have widely been used with the combination of

autoencoders, which can learn key features in an unsupervised manner while significantly reducing the number of dimensions of original input (Xu et al. 2015; Ribeiro et al. 2020). One of the most successful algorithms of this sort is Deep Support Vector Data Description (DSVDD) (Ruff et al. 2018), which learns a hyperspheric feature space where samples of an available class lie densely around a central point \vec{c} so that the distance from it is used as the indicator of novelty during test. We argue that the DSVDD distancing approach may oversimplify useful relationships among features for OC especially in high-dimensional spaces. Thus, we propose a generative module, *Inner-Outlier Generator* (*IO-GEN*), to replace the heuristic reference \vec{c} with synthesized “*inner outlier*” observations of an imaginary social-system state so that a separate classifier on DSVDD can use both the hyperspheric structure of data description and high-dimensional feature representation to learn behavioral abnormality.

We apply this IO-GEN approach to the analysis of a group of Indian jumping ants (*Harpegnathos saltator*), which typically show a *stable* (normal) state with mainly peaceful interactions. When the reproductive ants die or are artificially removed, the colony moves into a transient *unstable* (abnormal) state during which members go through a process that comes to consensus on a subset of workers that become the new reproductive individuals leading to a new stable state (Sasaki et al. 2016). There are conspicuous behavioral interactions that only occur during the unstable colony state, but a detailed understanding of how this transitory period is resolved remains elusive. We created a dataset for analysis by extracting optical flows from a colony of over 50 *H. saltator* ants to record their behavioral data for 20 days in a lab setting where the colony was artificially triggered to induce “stable–unstable–stable” colony state transitions. We then developed an approach following the simplified diagram in Fig. 1. Video data of a particular stable colony is used for normal-class training, and our proposed model then later assesses whether a focal colony is stable or unstable based on a short sequence of new optimal flow inputs.

Related Work

Behavioral Cues for Inferring Collective States

Inference and prediction of current and future collective states is potentially useful in a number of applications. In human crowds, intelligent surveillance cameras can detect abnormal collective states (e.g., conditions consistent with group-level panic or rioting behavior) (Mehran, Oyama, and Shah 2009) so that authorities can prioritize surveillance resources and execute proactive mitigation strategies. Alternatively, an individual robot in a multi-robot system can use local information of the pose of nearby robots to infer the large-scale formation of its team and then alter its own trajectory to more effectively achieve a group-level response to a stimulus encountered at distal ends of the team (Choi, Pavlic, and Richa 2017; Choi, Kang, and Pavlic 2020).

In behavioral ecology, however, modeling efforts have been focused either on the coarse-grained collective scale or the fine-grained individual scale but rarely the connection between the two. For example, many mathematical and

statistical models have been developed for understanding the evolution of group-level states and how they adapt to changes in the environment (Couzin et al. 2002; Reid et al. 2015; Sasaki et al. 2016; Pratt et al. 2002; Buhl et al. 2006). These approaches provide insights into the overall function of collective states but do not provide so much insight into how to map observations of an individual to the collective context of that individual. On the other end of the spectrum, more recent deep learning approaches for image segmentation or object detection have been tuned to track individual animals from video frames (Bozek et al. 2018; Nath et al. 2019). These efforts are focused on accelerating data acquisition for existing statistical pipelines that human researchers employ and not on making automated inferences across the individual–group scales. Calhoun, Pillow, and Murthy (2019) used an unsupervised learning framework to discover latent states in *Drosophila melanogaster* flies during courtship, but the inference scale was only limited to the group of two engaged flies while our work deals with much larger social groups (an entire animal society).

One-class Classification (OC) for Visual Data

Classical OC methods, such as One-class Support Vector Machine (OC-SVM) (Schölkopf et al. 2001) and Support Vector Data Description (SVDD) (Tax and Duin 2004), either use a hyperplane or a hypersphere tightly bounding the known-class data for separation. Recently, these methods have been augmented with autoencoders that highly reduce input dimensions of graphical data without supervision (Xu et al. 2015; Ribeiro et al. 2020). As an extension, DSVDD is designed to optimize the objective of SVDD in an end-to-end deep neural network pipeline (Ruff et al. 2018). In particular, the autoencoder’s encoder is fine-tuned to generate a feature space in which the in-class samples lie densely close to a pre-defined central vector \vec{c} , while the out-of-class samples are sparsely away from them (Fig. 2b). Although DSVDD showed competitive performance with several benchmark datasets, we argue that its distancing scheme – simply using the distance to \vec{c} – is not sufficiently rich to distinguish novel samples, and we combine DSVDD with a generative approach to improve OC for this case.

Generative Adversarial Networks (GANs) (Goodfellow et al. 2014) can also be used in OC by synthesizing fake outcomes consistent with typical samples that are then used in training to improve the generalizability of the OC (Sabokrou et al. 2018; Yadav, Chen, and Ross 2020; Perera, Nallapati, and Xiang 2019). However, these approaches adopt the conventional min–max scheme of GANs to closely emulate the data distribution of the available class (Fig. 2c) although the ultimate goal is to identify novel samples from a different distribution. Instead, our IO-GEN generates fake outcomes even closer to the idealized central vector \vec{c} (Fig. 2d). These more prototypical samples allow the subsequent classifier to learn sharper discrimination in the DSVDD feature space between normal and abnormal samples.

Background: *Harpegnathos saltator*

A key characteristic of an ant colony is a reproductive division of labor between reproductive and non-reproductive

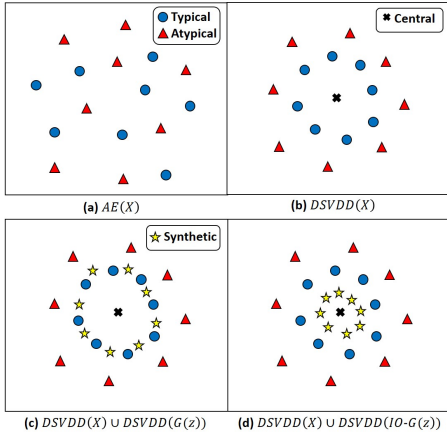


Figure 2: Conceptual feature formations in different methods on two-dimensional planes assuming only typical examples have been used for training each model. (a) The encoding from autoencoder cannot ensure a clear separation of atypical samples. (b) DSVDD forms the space in which data of seen class surround a central point \bar{c} more closely than unseen examples. (c) Generators in GANs learn to produce typical properties used for training. (d) IO-GEN synthesizes inner outliers much more densely to later substitute for \bar{c} .

individuals. In most ant colonies, a single “queen” is chiefly responsible for laying eggs that develop into non-reproductive “workers” that are responsible for caring for the next generation of eggs. Because workers typically cannot produce new workers themselves, the death of a queen usually means the expiration of the colony shortly after. In contrast, in the case of *H. saltator*, workers have the ability to produce all types of individuals including new workers, but they do not lay eggs while another reproductive is present. However, when there is no living reproductive in a colony, mated workers engage in a hierarchy reformation process lasting several weeks that terminates when several mated workers activate their ovaries and begin to produce eggs (Liebig, Peeters, and Hölldobler 1999; Sasaki et al. 2016). The reproductive ascendance of these workers, known as “gamergates” (Peeters and Crewe 1985), brings the colony back to a typical state. When those gamergates die or are removed, the instability will begin again (Liebig, Peeters, and Hölldobler 1999; Sasaki et al. 2016). During the unstable transient state, workers perform conspicuous aggressive behaviors such as *dueling*, *dominance biting*, and *policing* (Sasaki et al. 2016). Although these behaviors are clear signs that the colony is in this transient state, the precise combination of events that leads to a colony-level stable state remains unclear.

Dataset from Colonies in Transition

Deep-learning methods for image and video data have shown that optical flows can effectively complement classical RGB data in learning because they can extract transient behavioral characteristics (e.g., shooting) while RGB data largely provides an understanding of scenic context with vis-

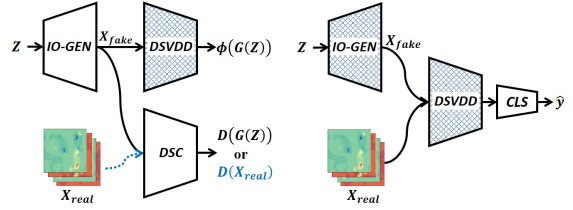


Figure 3: Training pipelines for IO-GEN (left) and Classifier (right). IO-GEN must meet two objectives simultaneously, one with the pre-trained DSVDD and one with the discriminator. Classifier learns binary classification on the data description that the DSVDD offers. Patterned components represent their parameters fixed during the training phase.

ible objects (e.g., bow and arrows) (Simonyan and Zisserman 2014). Because our framework only expects ants and crickets they feed upon in the scenes, we only use optical flows in our datasets so that learning will be based solely on behavioral flows, which is similar to the human-crowd behavior classification by Mehran, Oyama, and Shah (2009).

We used a colony of 59 *H. saltator* ants including 4 gamergates in a plastic nest covered by a transparent glass. Although an overhead camera filmed the nest, not all ants necessarily appear in all scenes because some may move to an off-camera foraging chamber through a tunnel on the left side of the nest. Videos were recorded for 20 days, denoted as D-2, D-1, D+1, ..., D+18, where D-0 represents the instant of removal of the previously identified gamergates between days 2 and 3 to artificially trigger the transient state of the colony. From D+1, we observed frequent *dueling* and *dominance biting* until the aggressiveness almost disappeared on the last several days across the group. By performing downsampling techniques, m sequential optical flows were sampled every 2 minutes, and, for each flow, a pair of horizontal and vertical motional representations in the spatial resolution of 64×64 were extracted from two consecutive frames with an interval of 0.5 seconds. The code provided by Wang et al. (2016) was used to acquire $1,333m$ stable-class and $11,984m$ unstable-class optical flows in total. Three unique splits of stable class were prepared to obtain the average performance of three separate models, as 80% and 20% were used for training and test, respectively in each split, while the unstable samples were included only in the test sets. All the data and split information are accessible online¹.

Methodology

DSVDD

DSVDD in our framework follows its original design from Ruff et al. (2018). It is built from the encoder part ϕ of a pre-trained autoencoder that is used to learn a feature space \mathcal{F} in which the samples of known class have a lower average distance to a central vector \bar{c} than those of novel class. Specifically, we adopt One-class DSVDD, which min-

¹https://github.com/ctyeong/OpticalFlows_HsAnts

imizes the objective:

$$\min_W \frac{1}{n} \sum_{i=1}^n \|\phi(x_i; W) - \vec{c}\|^2 + \frac{\lambda}{2} \sum_{l=1}^L \|W^l\|_F^2$$

where $\|\cdot\|_F$ is the Frobenius norm. The first term is closing the distance between \vec{c} and the feature representation of each sample x_i in encoder ϕ parameterized by W , and the second term is a weight decay regularizer for L layers with $\lambda > 0$. In the original method of DSVDD, the trained parameters $W = W^*$ are used to generate a distance:

$$s(x) = \|\phi(x; W^*) - \vec{c}\|^2$$

that is a proxy for how atypical a sample x is. For some threshold $\tau > 0$, $s(x) > \tau$ classifies x as atypical. Our method, however, substitutes the distancing heuristic $s(x)$ by IO-GEN and Classifier, described below, that we argue better utilize key features in the normal set in order to discriminate abnormal data after training.

IO-GEN

As shown in Fig. 3, IO-GEN G is designed to operate with both the pre-trained DSVDD ϕ and a discriminator network D , as a generative model of optical flows. With the discriminator, an adversarial learning is performed following the standard objective:

$$\min_G \max_D \left(\mathbb{E}_{z \sim N_\sigma} [\log(1 - D(G(z)))] + \mathbb{E}_{x \sim p} [\log(D(x))] \right)$$

where N_σ is the zero-mean normal distribution with standard deviation σ , and p is the probability distribution of real optical-flow data. Due to the first term, the outcomes from IO-GEN are adjusted to appear sufficiently realistic to deceive the discriminator. Also, the DSVDD is used to force the learned synthetic data to be inner outliers close to \vec{c} in \mathcal{F} , while the parameters of itself are not updated. In particular, we use the feature-matching technique proposed by Salimans et al. (2016), which incorporates the minimization:

$$\min_G \|\mathbb{E}_{z \sim N_\sigma} [\phi(G(z))] - \vec{c}\|_2^2$$

The composite loss function for IO-GEN is:

$$L_G = \mathbb{E}_{z \sim N_\sigma} [\log(1 - D(G(z)))] + \lambda \left(\|\mathbb{E}_{z \sim N_\sigma} [\phi(G(z))] - \vec{c}\|_2^2 \right)$$

where hyperparameter $\lambda > 0$ determines the relative weights between the two terms to minimize. In other words, IO-GEN is trained to produce ant behavioral flows that look real and also feature the closest proximity to \vec{c} in \mathcal{F} of DSVDD.

Classifier

Classifier utilizes real data from stable colony states as well as the generated IO-GEN inner outliers to learn to predict the likelihood of unstable behaviors on given m instant frame images as in general binary classifiers. We introduce a novel strategy, *label switch*, during training where the real stable samples are labelled as “unstable” (atypical) and the synthetic ones are labeled as “stable” (typical). This technique

leads the Classifier to eventually make low-, mid-, and high-range likelihood predictions for synthetic, stable, and unstable data, respectively, as though the augmented state of inner outliers was the “most stable” state . That is, Classifier offers likelihood outcomes somewhat consistent with the class distribution around \vec{c} allowing for a clear separation between real stable and unstable data, which will be demonstrated in the following sections.

Model Structures & Relevant Parameters

A Deep Convolutional Autoencoder (DCAE) is used as the backbone of DSVDD and IO-GEN once it has been trained with the data of stable class to minimize the reconstruction error in the Mean Squared Error (MSE) between the input encoded and the decoded output. Per input, m optical flows are all stacked one another to constitute an input $x \in \mathbb{R}^{64 \times 64 \times 2m}$ after normalization to range in $[-1, 1]$. In the encoder, three convolutional layers with 32, 64, and 128 2D kernels are employed in series as each kernel is of 3×3 size. Also, every output is followed by a *ReLU* activation and 2D maxpooling. The decoder has the reversed architecture of the encoder with two modifications: 2D upsampling instead of maxpooling and an added output layer with $2m$ kernels and *hyperbolic-tangent* (*tanh*) activation. An additional 32 convolutional kernels are placed as the encoder-decoder bottleneck to obtain a compact encoding scheme $\vec{v} \in \mathbb{R}^{1 \times 2048}$ when flattened. DSVDD takes advantage of the pre-trained encoder to reshape the space of \vec{v} by learning data description \mathcal{F} as the reference vector \vec{c} is the mean of available encoded samples according to Ruff et al. (2018).

IO-GEN essentially employs a fully connected layer with the *ReLU* activation that takes a noisy vector $\vec{z} \in \mathbb{R}^{1 \times 100}$ as input. It is then connected to a replica of the pre-trained decoder so that realistic synthesis can be learned faster from the prior knowledge of reconstruction. The discriminator network builds an extra fully connected layer with a *sigmoid* activation on top of encoder, but its weights are all reinitialized because otherwise it appears to easily overwhelm IO-GEN in performance causing unstable adversarial training. Also, $\lambda = 10$ was empirically found most effective to minimize L_G .

Because Classifier comes after DSVDD, it has an independent architecture in which five convolutional layers learn 8, 16, 24, 48, and 48 one-dimensional kernels, respectively. Each layer has a *LeakyReLU* activation ($\alpha = 0.3$) and 1D average pooling, and lastly, a fully connected layer is deployed to provide a predicted likelihood of unstable state via a *sigmoid* function. All codes are also available online².

Experiments

Observations of Optical Flow Weights

We first attempt to make use of the optical flow dataset to discover insightful motional patterns without any complex model. As with Mahasseni et al. (2013), we compute an optical flow weight w_i for each frame i by averaging the magnitudes of flow vectors at all locations. Figure 4 displays the

²<https://github.com/ctyeong/IO-GEN>

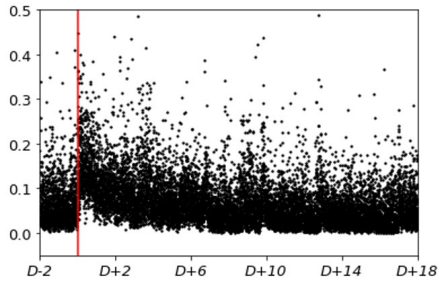


Figure 4: Optical flow weights each sampled at the interval of over 2 minutes for 20 days. The horizontal axis shows the days of observation with the red separator when the *gamergates* were intentionally moved. The vertical axis indicates the weight levels, each standardized in $[0, 1]$ by the global max and min, omitting extreme outliers for clarity.

obtained weight signal in time as $m = 1$ optical flow frame is considered for each sampling interval.

For the first two days, the weights generally stay in a narrow range implying some behavioral regularity maintained among ants. Then there is a noticeable increase in weights starting at D+1 just after the gamergates are removed because the removal triggered a social tournament involving frequent aggressive behaviors. As the transient period evolves, the magnitude continues to decrease and finally recovers the original extent roughly on D+10 even though several ants continue to present hostile interactions at that time.

Consequently, a simple model might be built that uses the overall rise of flow weight as the only feature to distinguish the unstable colony from the stable especially at early development of the unstable state. However, following our results, we will provide concrete examples that show the limitations of such a design and the need of more complex models for reliable predictions.

Model Evaluation

Here, we demonstrate the OC performance of our proposed method. We first describe an ablation study to find the best number of optical-flow frames per input. Next, baselines used for comparison are introduced that will help us explore our method’s overall reliability and prediction robustness in various time windows during colonial stabilization.

As in previous works (Ruff et al. 2018), the Area Under the Curve (AUC) of the Receiver Operating Characteristics (ROC) are measured for each model to reflect the separability between classes. Moreover, the average over three splits is reported with the standard deviation when needed.

Ablation Study: Results from tests with $m \in \{1, 2, 4\}$ are shown in Table 1. There was an improvement as m increased from 1 to 2, while doubling it to 4 did not offer any benefit. The result may indicate that the observation of one more second does not add significantly more information. Learning IO-GEN could also be more challenging as it is asked to generate longer motional sequences. Thus, m is set to 2 hereafter considering both efficiency and effectiveness of our model.

m	1	2	4
AUC	0.760 ± 0.016	0.786 ± 0.009	0.787 ± 0.008

Table 1: Average performance when the number of optical flow image frames per input is set to 1, 2, or 4.

METHOD	AUC
OFW	0.506
DCAE	0.506 ± 0.002
OC-SVM	0.523 ± 0.004
DSVDD	0.762 ± 0.013
GEN	0.587 ± 0.032
N-GEN	0.699 ± 0.006
IO-GEN	0.786 ± 0.009

Table 2: Average AUC of tested models with the standard deviation as all 18-day unstable observations are considered.

Baselines: **OFW** uses the temporal optical flow weights to set the best threshold to report the best classification result. **DCAE** is a similar threshold-based method relying on the reconstruction error as the feature of novelty (Kerner et al. 2019). **OC-SVM** (Schölkopf et al. 2001) takes the encoder of DCAE to build the One-class SVM on it providing the performance with the best v parameter. While **DSVDD** here is designed similarly to the description by Ruff et al. (2018), the adjustments in our implementation are described in Model Structures & Relevant Parameters above. **GEN** and **N-GEN** are generative models to train a separate classifier as our method. GEN is, however, a standard generative model adopting the feature matching technique in the discriminator network instead without the intervention of DSVDD. N-GEN replaces $\phi(G(z))$ with arbitrary noisy data $\vec{v}' \in \mathbb{R}^{1 \times 2048}$ where each element of \vec{v}' is drawn from $N(0, \alpha)$ where α is the global variation of $\vec{v} \sim \phi(G(z))$.

Overall Performance: Table 2 helps estimate overall reliability of each model for the image inputs that can be captured at an arbitrary timing since all samples from unstable colony were included for test. OFW and DCAE suggest the limitation of only relying on thresholding a simplistic one-dimensional signal. In particular, the low accuracy of DCAE implies that precise reconstruction is achieved also for the motions from unseen, unstable colony. Similarly, the OC-SVM can utilize only little benefit from the encoding capability. On the other hand, DSVDD leads at least 45% increase of AUC score simply fine-tuning the encoder part of DCAE because unstable examples are more easily distinguished in the newly learned hyperspheric data description. In addition, our model brings about a further improvement proving that utilizing a subsequent classifier with synthetic examples can be more effective than the distancing heuristic in DSVDD to make full use of multi-dimensional relationships among features. Nevertheless, GEN and N-GEN provide 25% and 11% poorer performance than ours although both also use synthetic data to train a classifier. N-GEN

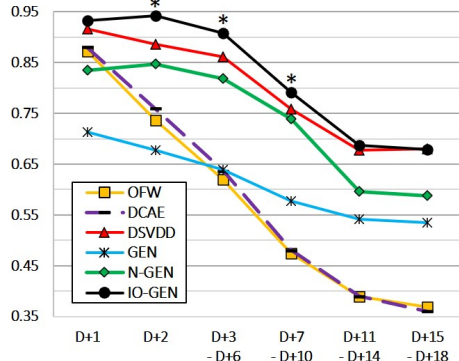


Figure 5: Average AUC changes for predictions within different temporal windows. Asterisks (*) mark statistically significant improvement over DSVDD ($p < .05$).

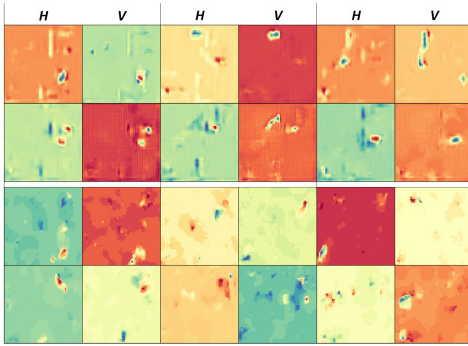


Figure 6: Optical flow examples: (top two rows) Six synthesized pairs from IO-GEN; (bottom two rows) Six real examples. Each (H-V) pair show horizontal and vertical motions, respectively, for which pixels are normalized in each image.

actually performs better than GEN implying that the prior knowledge on data description is useful for effective data synthesis. Still, its insufficient reliability emphasizes the importance of realism in generated datasets as well.

Detection in Different Developmental Phases: Figure 5 displays the performance variation of each model as the tested data from the unstable colony are confined in various temporal windows. Consistent with Fig. 4, the prediction performance generally degrades for later temporal bins because the ant colony is more stabilized. Our framework still indicates the top performance in almost any phase especially presenting the highest margins from DSVDD in a highly ambiguous time period between D+2 and D+10, in which the proportion of stable observations dramatically increased. As expected from Fig. 4, OFW and DCAE highly depend on the timing of application because their scores are close to that of DSVDD early while lower even than 0.5 after D+6. If the initial social transition is less conspicuous, possibly due to a smaller population, these models may perform poorly because of less intense competition caused. Moreover, the results from GEN and N-GEN reemphasize the insufficiency of solely relying on realism or spatial character-

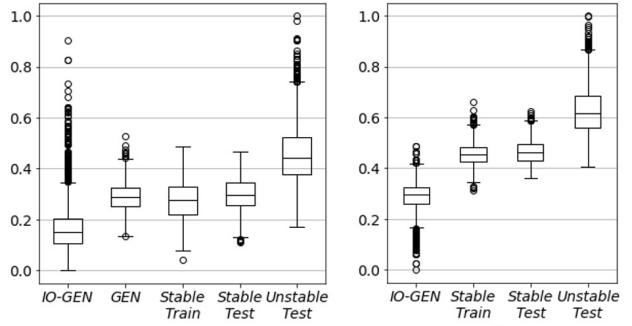


Figure 7: For different types of data: On left, normalized Euclidean distances to \bar{c} in feature description \mathcal{F} of DSVDD. On right, predicted likelihoods from Classifier.

istics of produced features when training generative models. In particular, as illustrated in Fig. 2, GEN produces fake samples that closely resemble the ones of stable state, and so the biased classifier leads to the worst performance in the early stages ($\sim D+2$) when colonial instability was highest.

Model Properties

Figure 6 compares synthetic optical flows from IO-GEN to real optical flows; the generated optical flows are visually similar to real flows. Furthermore, Fig. 7a illustrates that the lowest distance distribution to \bar{c} is measured with IO-GEN, as designed, whereas GEN behaves similarly to the stable dataset. Figure 7b finally shows the predictive outcomes of Classifier, which are likelihoods of unstable state. With the *label switch*, the confidence becomes positively correlated with the distance to \bar{c} viewing inner outliers as samples from the most stable colony. Clear differences between classes imply that learned knowledge to discriminate stable and more-stable states in DSVDD can be transferred for classification of another pair as stable or unstable.

Conclusion

We have introduced a novel generative model IO-GEN that can utilize a pre-trained DSVDD and a separate classifier to successfully solve the OC problem. Our framework has been applied to 20-day video data from an entire society of 59 *H. saltator* ants to identify a colony’s stable or unstable state only from a 1-second motional sequence. Experiments have shown that the classifier trained with the synthetic data from IO-GEN outperforms other state-of-the-art baselines at any temporal phase during social stabilization.

Our future directions include a graphical user interface for this method that acts as a tool for biologists that can propose frames or individuals (regions of interest) implicated as being crucial in the evolution of social state. To implement this, an additional module can be built to monitor and visualize the levels of gradient passing from spatio-temporal behavioral features to the final decision output (Choi 2020).

Acknowledgments

Support provided by NSF PHY-1505048 and SES-1735579.

References

- Bozek, K.; Hebert, L.; Mikheyev, A. S.; and Stephens, G. J. 2018. Towards dense object tracking in a 2D honeybee hive. In *Proc. IEEE CVPR 2018*, 4185–4193.
- Buhl, J.; Sumpter, D. J.; Couzin, I. D.; Hale, J. J.; Despland, E.; Miller, E. R.; and Simpson, S. J. 2006. From disorder to order in marching locusts. *Science* 312(5778): 1402–1406.
- Calhoun, A. J.; Pillow, J. W.; and Murthy, M. 2019. Unsupervised identification of the internal states that shape natural behavior. *Nature Neuroscience* 22(12): 2040–2049.
- Choi, T. 2020. *Deep Learning Approaches for Inferring Collective Macrostates from Individual Observations in Natural and Artificial Multi-Agent Systems Under Realistic Constraints*. Ph.D. thesis, Arizona State University.
- Choi, T.; Kang, S.; and Pavlic, T. P. 2020. Learning local behavioral sequences to better infer non-local properties in real multi-robot systems. In *Proc. ICRA 2020*.
- Choi, T.; Pavlic, T. P.; and Richa, A. W. 2017. Automated synthesis of scalable algorithms for inferring non-local properties to assist in multi-robot teaming. In *Proc. IEEE CASE 2017*, 1522–1527.
- Couzin, I. 2007. Collective minds. *Nature* 445(7129): 715–715.
- Couzin, I. D.; Krause, J.; James, R.; Ruxton, G. D.; and Franks, N. R. 2002. Collective memory and spatial sorting in animal groups. *J. Theor. Biol.* 218(1): 1–12.
- Goodfellow, I.; Pouget-Abadie, J.; Mirza, M.; Xu, B.; Warde-Farley, D.; Ozair, S.; Courville, A.; and Bengio, Y. 2014. Generative adversarial nets. In *Proc. NIPS 2014*, 2672–2680.
- Heinze, J.; Hölldobler, B.; and Peeters, C. 1994. Conflict and cooperation in ant societies. *Naturwissenschaften* 81(11): 489–497.
- Kerner, H. R.; Wellington, D. F.; Wagstaff, K. L.; Bell, J. F.; Kwan, C.; and Amor, H. B. 2019. Novelty detection for multispectral images with application to planetary exploration. In *Proc. AAAI 2019*, volume 33, 9484–9491.
- Liebig, J.; Peeters, C.; and Hölldobler, B. 1999. Worker policing limits the number of reproductives in a ponerine ant. *Proc. R. Soc. B* 266(1431): 1865–1870.
- Mahasseni, B.; Chen, S.; Fern, A.; and Todorovic, S. 2013. Detecting the Moment of Snap in Real-World Football Videos. In *Proc. IAAI 2013*.
- Mehran, R.; Oyama, A.; and Shah, M. 2009. Abnormal crowd behavior detection using social force model. In *Proc. IEEE CVPR 2009*, 935–942.
- Nath, T.; Mathis, A.; Chen, A. C.; Patel, A.; Bethge, M.; and Mathis, M. W. 2019. Using DeepLabCut for 3D markerless pose estimation across species and behaviors. *Nature Protocols* 14(7): 2152–2176.
- Peeters, C.; and Crewe, R. 1985. Worker reproduction in the ponerine ant *Ophthalmopone berthoudi*: an alternative form of eusocial organization. *Behavioral Ecology and Sociobiology* 18(1): 29–37.
- Perera, P.; Nallapati, R.; and Xiang, B. 2019. Ocgan: One-class novelty detection using gans with constrained latent representations. In *Proc. IEEE CVPR 2019*, 2898–2906.
- Pratt, S. C.; Mallon, E. B.; Sumpter, D. J.; and Franks, N. R. 2002. Quorum sensing, recruitment, and collective decision-making during colony emigration by the ant *Leptothorax albipennis*. *Behav. Ecol. Sociobiol.* 52(2): 117–127.
- Reid, C. R.; Lutz, M. J.; Powell, S.; Kao, A. B.; Couzin, I. D.; and Garnier, S. 2015. Army ants dynamically adjust living bridges in response to a cost–benefit trade-off. *Proc. Natl. Acad. Sci. USA* 112(49): 15113–15118.
- Ribeiro, M.; Gutoski, M.; Lazzaretti, A. E.; and Lopes, H. S. 2020. One-Class Classification in Images and Videos Using a Convolutional Autoencoder With Compact Embedding. *IEEE Access* 8: 86520–86535.
- Ruff, L.; Vandermeulen, R. A.; Görnitz, N.; Deecke, L.; Siddiqui, S. A.; Binder, A.; Müller, E.; and Kloft, M. 2018. Deep one-class classification. In *Proc. ICML 2018*, volume 10, 6981–6996.
- Sabokrou, M.; Khalooei, M.; Fathy, M.; and Adeli, E. 2018. Adversarially learned one-class classifier for novelty detection. In *Proc. IEEE CVPR 2018*, 3379–3388.
- Salimans, T.; Goodfellow, I.; Zaremba, W.; Cheung, V.; Radford, A.; and Chen, X. 2016. Improved techniques for training gans. In *Proc. NIPS 2016*, 2234–2242.
- Sasaki, T.; Penick, C. A.; Shaffer, Z.; Haight, K. L.; Pratt, S. C.; and Liebig, J. 2016. A simple behavioral model predicts the emergence of complex animal hierarchies. *The American Naturalist* 187(6): 765–775.
- Schölkopf, B.; Platt, J. C.; Shawe-Taylor, J.; Smola, A. J.; and Williamson, R. C. 2001. Estimating the support of a high-dimensional distribution. *Neural Computation* 13(7): 1443–1471.
- Simonyan, K.; and Zisserman, A. 2014. Two-stream convolutional networks for action recognition in videos. In *Proc. NIPS 2014*, 568–576.
- Tax, D. M.; and Duin, R. P. 2004. Support vector data description. *Machine Learning* 54(1): 45–66.
- Wang, L.; Xiong, Y.; Wang, Z.; Qiao, Y.; Lin, D.; Tang, X.; and Van Gool, L. 2016. Temporal segment networks: Towards good practices for deep action recognition. In *European conference on computer vision*, 20–36.
- Xu, D.; Ricci, E.; Yan, Y.; Song, J.; and Sebe, N. 2015. Learning deep representations of appearance and motion for anomalous event detection. *arXiv preprint arXiv:1510.01553*.
- Yadav, S.; Chen, C.; and Ross, A. 2020. Relativistic Discriminator: A One-Class Classifier for Generalized Iris Presentation Attack Detection. In *The IEEE Winter Conference on Applications of Computer Vision*, 2635–2644.